Supporting information

S1. Potential parameters

The interatomic potential parameters for lattice ions are listed in Table S1. The potential parameters for Ti^{4+}-O^{2-} were taken directly from previous simulations of $BaTiO_3$, which were derived by G. V. Lewis and C. R. A. Catlow by a least squares fitting procedure to experimentally known crystal properties of TiO_2.[1] The short range potential parameters and the shell-model parameters for Na^{+}-O^{2-} used in this study were derived by J. R. Tolchard *et al*.[2] The potential parameters for Bi^{3+}-O^{2-} were taken from M. E. G. Valerio *et al* in a study of $Bi_4Ge_3O_{12}$ and R. A. Jackson *et al* in a study of $Bi_4Ti_3O_{12}$.[3,4] The potential parameters for Bi^{3+}-O^{2-} and O^{2-}-O^{2-} were refined by fitting to the experimental structure parameters of NBT, including cubic ($Fm\bar{3}m$), rhombohedral ($R3c$) and monoclinic (Cc). The well reproduction of the rather complex crystal structures of NBT demonstrates the reliability of the potential parameters and the subsequent defect, dopant, and migration simulations.

Table S1 Interatomic potential parameters and binary oxide lattice energies calculated using the same O^{2-}-O^{2-} potential.

	Buckingham parameters			Shell model parameters		Lattice energy for binary oxide (eV)
M-O^{2-}	*A* / eV	*ρ* / Å	*C* / eV Å^6	*Y* / e	*k* / eV Å^{-2}	
Na^{+}-O^{2-}	611.10	0.3535	0	1.0	99999	-24.90
Bi^{3+}-O^{2-}	3265.681	0.3305	18.25	-2.0	145	-125.30
Ti^{4+}-O^{2-}	877.2	0.38096	9.0	-35.863	65974.0	-111.93
O^{2-}-O^{2-}	22764.3	0.149	27.88	-2.67	74.92	-

S2. Formation of intrinsic defects

1) Oxygen-vacancy formation energies

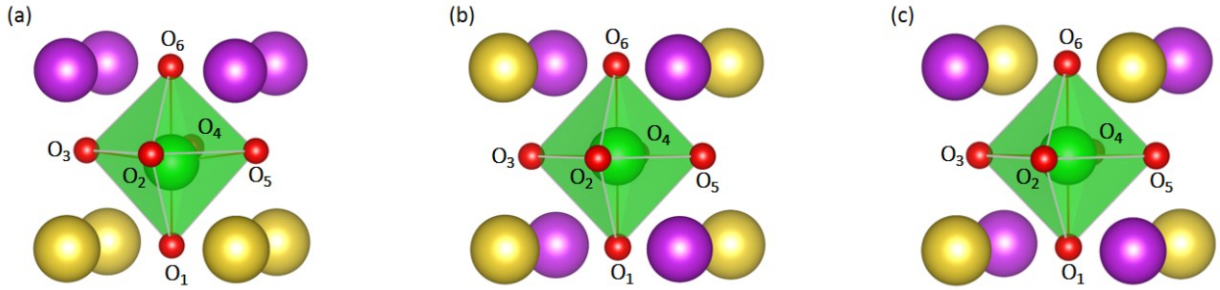

Fig. S1 Illustration of oxide ions with different chemical environments in (a) (100)-, (b) (110)- and (c) (111)-ordered cubic NBT. Key: Na (yellow); Bi (purple); Ti (green); oxygen (red).

The chemical environments of oxide ions in different chemical ordered structures are illustrated in Fig. S1 and the corresponding oxygen-vacancy formation energies are listed in Table S2. There are three distinct binding environments for oxide ions in the (100)-ordered structure: bonded to four Na cations (O_1), bonded to two Na and two Bi cations (O_2, O_3, O_4 and O_5) and bonded to four Bi cations (O_6). The lowest oxygen-vacancy formation energy (17.47 eV) is observed for oxide ion with four Bi coordination (O_6), while the highest oxygen-vacancy formation energy is for oxygen (O_1) with four Na coordination (18.68 eV). These results are consistent with experimental results, revealing the weak bonding

nature of the Bi-O bonds.[5, 6] Therefore, oxygen-vacancies are much easier to form in Bi rich regions. This is further confirmed by the (110)-ordered structure: although all the oxide ions have similar coordination (2 Bi and 2 Na), O_2, O_3, O_4 and O_5 (in a layer perpendicular to the Bi columns and Na columns) have longer Na-O bond (2.93 Å) but shorter Bi-O bond (2.72 Å) than that of O_1 and O_6 (in a layer parallel to the Bi columns and Na columns), (2.83 Å for all the Na-O and Bi-O bonds). Therefore, the oxygen-vacancy formation energy for O_2, O_3, O_4 and O_5 (17.95 eV) are lower than O_1 and O_6 (18.38 eV). All the oxide ions in the (111)-ordered structure have the same chemical environment (2 Bi and 2 Na for each) and the same Na-O and Bi-O bond length (2.81 Å) and therefore all the oxide ions have the same vacancy formation energy (17.95 eV).

Table S2 Calculated oxygen-vacancy formation energies for cubic NBT with different chemical ordered structures.

Chemical order	O_1	O_2	O_3	O_4	O_5	O_6
100	18.68	17.77	17.77	17.77	17.77	17.47
110	18.38	17.95	17.95	17.95	17.95	18.38
111	17.95	-	-	-	-	-

2) Formation of Frenkel and Schottky disorders

By combing the individual defect energies and the lattice energies, the intrinsic defect energies including the Frenkel disorder, partial Schottky disorder and full Schottky disorder were calculated. The defect reactions are given below:

Bismuth Frenkel disorder:

$$Bi_{Bi}^{\times} \rightarrow V_{Bi}''' + Bi_i^{\bullet\bullet\bullet}$$

Sodium Frenkel disorder:

$$Na_{Na}^{\times} \rightarrow V_{Na}' + Na_i^{\bullet}$$

Titanium Frenkel disorder:

$$Ti_{Ti}^{\times} \rightarrow V_{Ti}'''' + Ti_i^{\bullet\bullet\bullet\bullet}$$

Oxygen Frenkel disorder:

$$O_O^{\times} \rightarrow V_O^{\bullet\bullet} + O_i''$$

Bi_2O_3 partial Schottky disorder:

$$2Bi_{Bi}^{\times} + 3O_O^{\times} \rightarrow 2V_{Bi}''' + 3V_O^{\bullet\bullet} + Bi_2O_3$$

Na_2O partial Schottky disorder:

$$2Na_{Na}^{\times} + O_O^{\times} \rightarrow 2V_{Na}' + V_O^{\bullet\bullet} + Na_2O$$

TiO_2 partial Schottky disorder:

$$Ti_{Ti}^{\times} + 2O_O^{\times} \rightarrow V_{Ti}'''' + 2V_O^{\bullet\bullet} + TiO_2$$

$(Na_{0.5}Bi_{0.5})TiO_3$ full Schottky disorder:

$$\frac{1}{2}Bi_{Bi}^{\times} + \frac{1}{2}Na_{Na}^{\times} + Ti_{Ti}^{\times} + 3O_O^{\times} \rightarrow \frac{1}{2}V_{Bi}''' + \frac{1}{2}V_{Na}' + V_{Ti}'''' + 3V_O^{\bullet\bullet} + (Na_{0.5}Bi_{0.5})TiO_3$$

The calculated intrinsic defect energies are listed in Table S3. The Frenkel disorder energies are much higher than the other disorder energies. Therefore, interstitials would be unlikely intrinsic defects (as would be expected in a closed packed perovskite structure). It is noted that the exact intrinsic defect configuration is chemical order dependent: the most favourable energy corresponds to the formation of Na_2O partial Schottky (1.67 eV), NBT full Schottky (1.82 eV) and Bi_2O_3 partial Schottky (0.95 eV) for the (100)-, (110)- and (111)-ordered structures, respectively. Therefore, high concentration of Bi_2O_3 and Na_2O partial Schottky in NBT are expected, especially at the surface and interfaces.

Table S3 Calculated formation energies for Frenkel- and Schottky-type disorders (in eV per defect) for cubic NBT with different chemical ordered structures.

Chemical order	Bi Frenkel	Na Frenkel	Ti Frenkel	O Frenkel	Bi_2O_3 partial Schottky	Na_2O partial Schottky	TiO_2 partial Schottky	NBT full Schottky
(100)	7.78	2.53	6.98	3.63	2.29	1.67	2.71	2.37
(110)	3.83	2.04	4.38	4.05	1.89	2.11	2.11	1.82
(111)	6.27	3.86	3.88	[a]NC	0.95	2.42	1.15	1.08

[a]NC: Non-convergence of calculation

S3. MSDs of cations

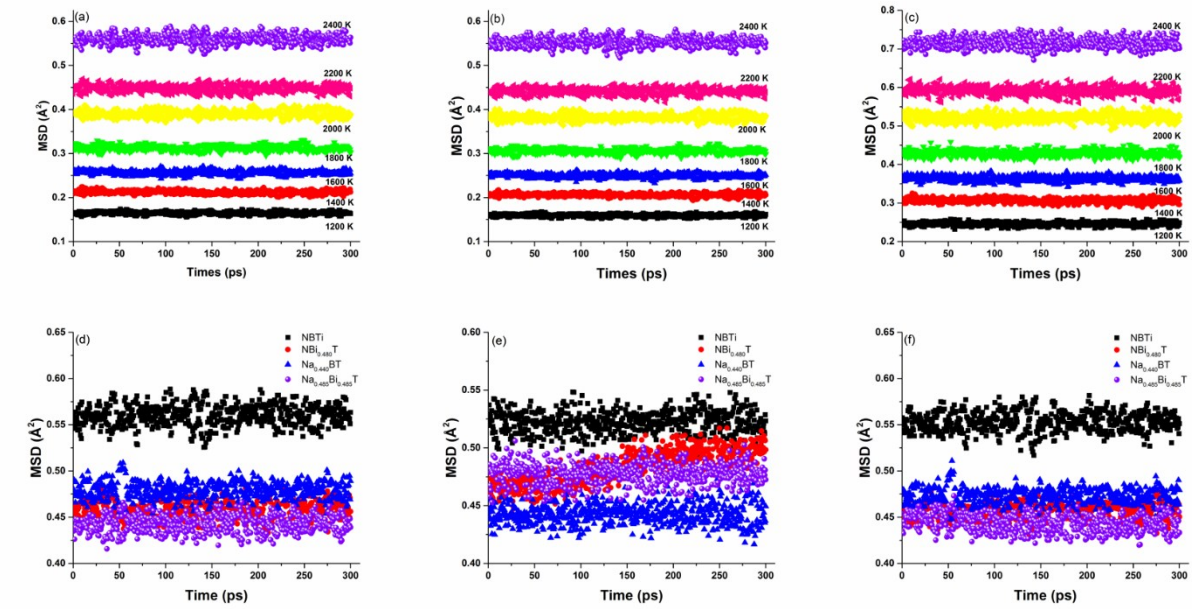

Fig. S2 The up panel: the MSDs of (a) Bi^{3+}; (b) Na^{+} and (c) Ti^{4+} for NBTi as a function of temperature. The down panel: the MSDs of (d) Bi^{3+}; (e) Na^{+} and (f) Ti^{4+} for NBTi, $NBi_{0.480}T$, $Na_{0.440}BT$ and $Na_{0.485}Bi_{0.485}T$ at 2400 K.

S4. Migration of Bi^{3+}/Na^{+} cations in the (110)- and (111)-ordered structures

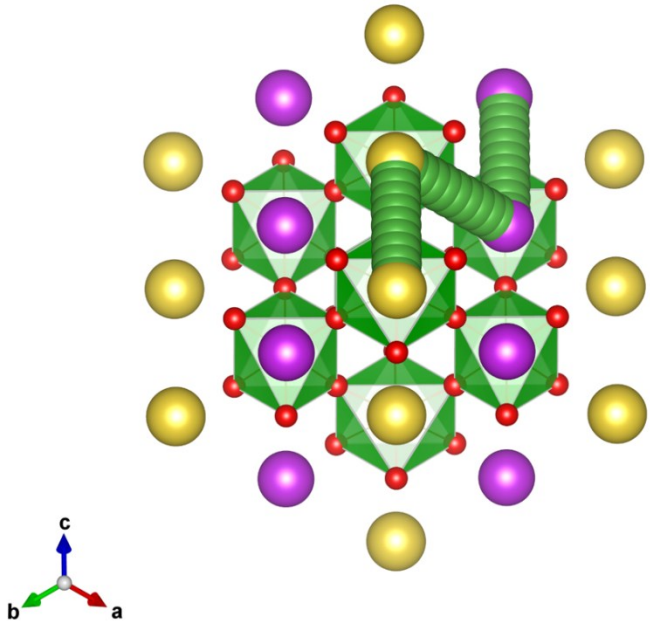

Fig. **S3** Traced trajectories for different migration mechanisms of Bi^{3+}/Na^{+} in the (110)-ordered structure: migration within a Na column; migration from a Na column to a Bi column and *vice versa* and migration within a Bi column. The Bi^{3+} and Na^{+} cations follow linear pathways.

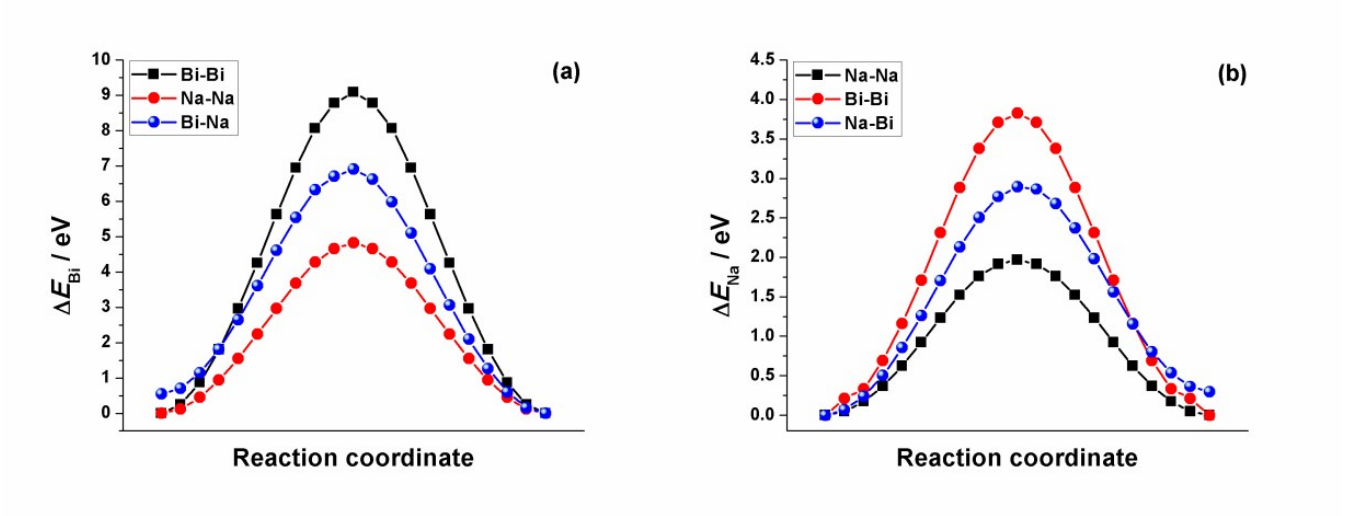

Fig. **S4** Energy profiles for (a) Bi^{3+} and (b) Na^{+} along different diffusion pathways in the (110)-ordered structure from its lattice site to a vacant site. Bi-Bi denotes the migrations of Bi^{3+}/Na^{+} within a Bi column; Na-Na denotes the migrations of Bi^{3+}/Na^{+} within a Na column; Bi-Na denotes the migrations of Bi^{3+} from a Bi column to a Na column; Na-Bi denotes the migrations of Na^{+} from a Na column to a Bi column. The first point on the left side in (a) is a Bi site, whilst in (b) the first point on the left side is a Na site.

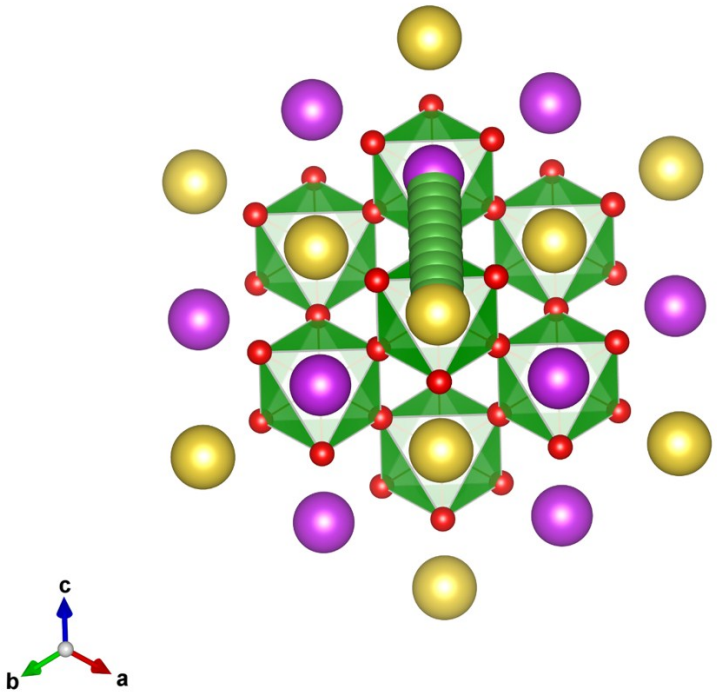

Fig. **S5** Traced trajectory for Bi^{3+}/Na^{+} to migrate from a Bi site to a Na site and *vice versa* in the (111)-ordered structure, which shows that both Bi^{3+} and Na^{+} cations follow a linear pathway.

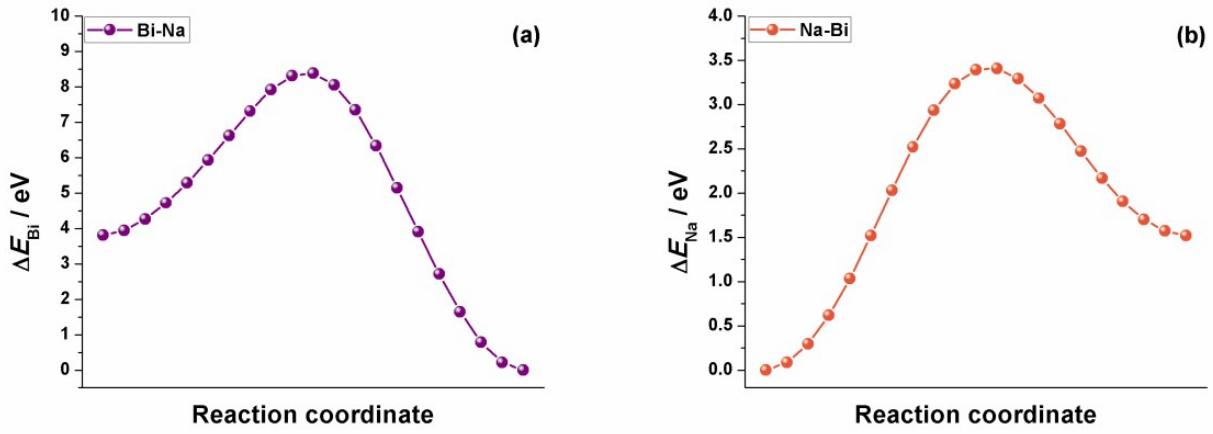

Fig. **S6** Energy profiles for (a) Bi^{3+} and (b) Na^{+} in the (111)-ordered structure. The first point on the left side in (a) is a Bi site, whilst in (b) the first point on the left side is a Na site.

S5. Ionic migration in Bi^{3+}/Na^{+} randomly distributed structure.

The ionic migration in Bi^{3+}/Na^{+} randomly distributed structure was investigated using a "mean-field approach". This was realized by defining a hybrid atom, which is consisted of half Bi^{3+} and half Na^{+}, occupying each of the *A*-site. Thus, the short-range interaction between the hybrid atom and the oxide ion (V_{hybrid}) can be expressed by the following equation:

$$V_{\text{Hybrid}} = \frac{1}{2}V_{\text{Bi}^{3+}\text{L O}^{2-}} + \frac{1}{2}V_{\text{Na}^{+}\text{L O}^{2-}} \qquad (1)$$

This feature allows the simulation of the ionic migration in the structure with randomly distribution of Bi^{3+} and Na^{+} cations. Thus, the energy barriers can be viewed as the average energy barrier of ionic migrations along different diffusion pathways in Bi^{3+}/Na^{+} ordered structures. The energy barriers for Bi^{3+} and Na^{+} to migrate from a lattice site to an adjacent vacant site are computed to be 6.70 and 2.75 eV, respectively. Meanwhile, the energy barrier for Ti^{4+} to migrate along the $[100]_{cubic}$ direction is found to be 7.07 eV. These energy barriers are much higher than the migration of oxide ion (0.67 eV) and further demonstrate the low level of cation conductivity to the total high ionic conductivity.

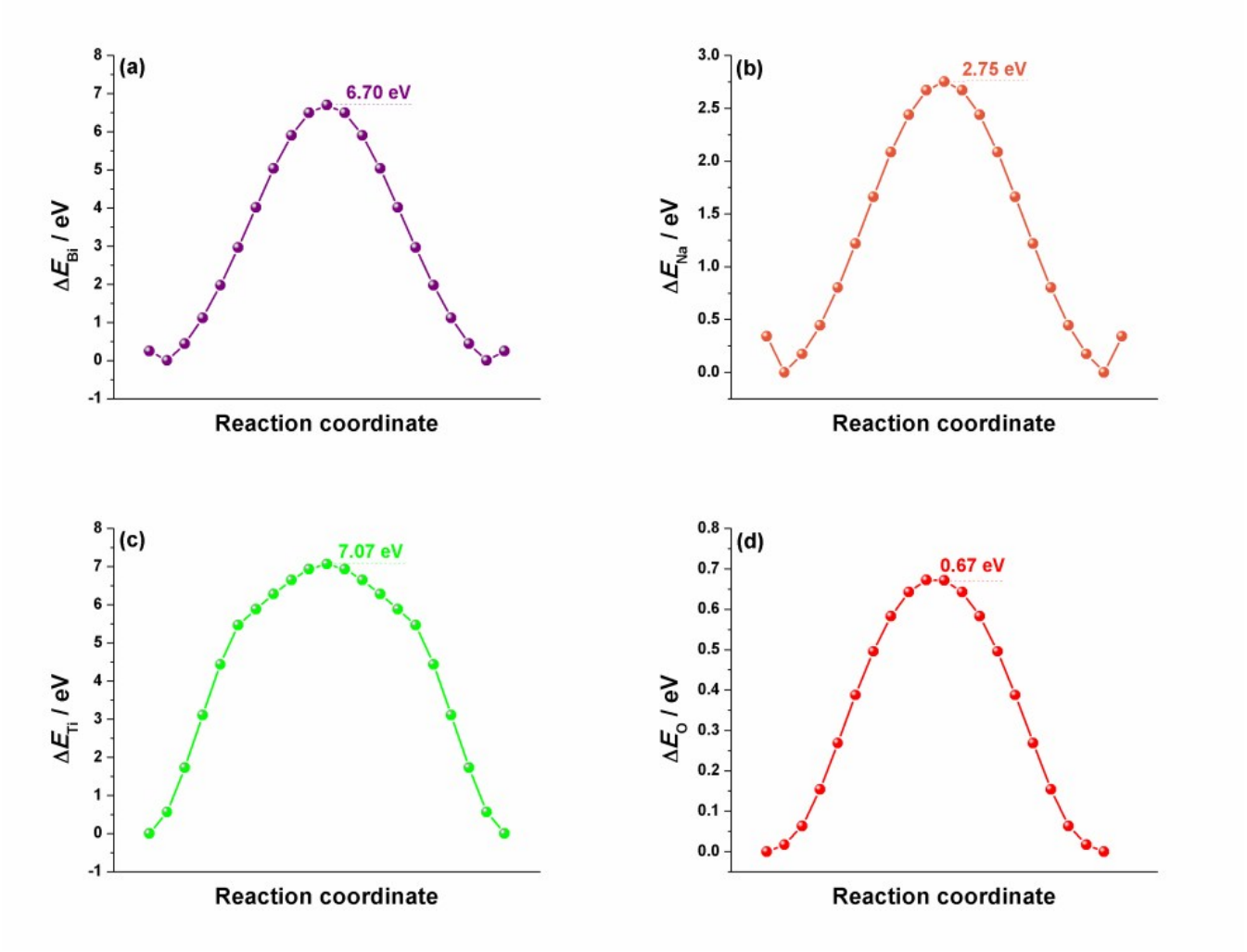

Fig. **S7** Energy profiles for (a) Bi^{3+}, (b) Na^{+}, (c) Ti^{4+} and (d) O^{2-} in Bi^{3+}/Na^{+} randomly distributed cubic NBT. The energy profile for Ti^{4+} corresponds to the migration along the $[100]_{cubic}$ direction. Note that the lowest energies for Bi^{3+} and Na^{+} are found at positions near to their ideal (hybrid atom) positions. This is because Bi^{3+} and Na^{+} can be viewed as impurities in this structure and therefore they will rattle around the ideal positions.

References

1 G. V. Lewis and C. R. A. Catlow, *J. Phys. Chem. Solids.*, 1986, **47**, 89-97.

2 J. R. Tolchard, P. R. Slater and M. S. Islam, *Adv. Funct. Mater.*, 2007, **17**, 2564-2571.

3 M. E. Valerio, R. A. Jackson and Z. S. Macedo, *Phys. Stat. Sol.(c)2*, 2005, **1**, 485-489.

4 R. A. Jackson, J. A. Dawson, M. E. G. Valerio and Z. S. Macedo, *Opt. Mater.*, 2010, **32**, 1375-1376.

5 D. Schütz, M. Deluca, W. Krauss, A. Feteira, T. Jackson, K. Reichmann, *Adv. Funct. Mater.*, 2012, **22**, 2285-2294.

6 P. D. Battle, C. R. A. Catlow, J. W. Heap and L. M. Moroney, *J. Solid State Chem.*, 1987, **67**, 42-50.